Biosensors and Bioelectronics 207 (2022) 114195

Contents lists available at ScienceDirect

Biosensors and Bioelectronics

journal homepage: www.elsevier.com/locate/bios

In situ, real-time, colorimetric detection of γ-hydroxybutyric acid (GHB) using self-protection products coated with chemical receptor-embedded hydrogel

Siyoung Ha [a,1], Jinyeong Kim [a,1], Chul Soon Park [a,f], Sangwoo Lee [b], Donggon Yoo [b,c], Kyung Ho Kim [a], Sung Eun Seo [a], Seon Joo Park [a], Jai Eun An [a], Hyun Seok Song [d], Joonwon Bae [e], Woo-Keun Kim [b,c,**], Oh Seok Kwon [a,g,*]

[a] Infectious Disease Research Center, Korea Research Institute of Bioscience and Biotechnology, Daejeon, 34141, Republic of Korea
[b] Biosystem Research Lab, Korea Institute of Toxicology, Daejeon, 34114, Republic of Korea
[c] Human and Environmental Toxicology, University of Science and Technology, Daejeon, 34113, Republic of Korea
[d] Sensor System Research Center, Korea Institute of Science and Technology, Seoul, 02792, Republic of Korea
[e] Department of Applied Chemistry, Dongduk Women's University, Seoul, 02748, Republic of Korea
[f] Process Development Team, Drug Manufacturing Center, Daegu-Gyeongbuk Medical Innovation Foundation (DGMIF), Daegu, 41061, Republic of Korea
[g] Nanobiotechnology and Bioinformatics (Major), University of Science & Technology (UST), 125 Gwahak-ro, Yuseong-gu, Daejeon, 34141, Republic of Korea

ARTICLE INFO

Keywords:
γ-Hydroxybutyric acid(GHB)
Drug-facilitated sexual assault(DFSA)
Self-protection product(SPP)
In-situ colorimetric detection
Chemical receptor

ABSTRACT

Due to the increase in drug-facilitated sexual assault (DFSA) enabled by the illegal use of drugs, there have been constant demands for simple methods that can be used to protect oneself against crime in real life. γ-Hydroxybutyric acid (GHB), a central nervous system depressant, is one of the most dangerous drugs for use in DFSA because it is colorless and has slow physiological effects, which pose challenges for developing in situ, real-time GHB monitoring techniques. In this study, we developed a method for in situ colorimetric GHB detection using various self-protection products (SPPs) coated with 2-(3-bromo-4-hydroxystyryl)-3-ethylbenzothiazol-3-ium iodide (BHEI) as a chemical receptor embedded in hydrogels. Additionally, smartphone-based detection offers enhanced colorimetric sensitivity compared to that of the naked eye. The developed SPPs will help address drug-facilitated social problems.

1. Introduction

Pain relief and memory loss are hallmarks of dissociative anesthetics. Sensory disturbances and improper communication of the nervous system create a state of disconnection of the mind from the body (Tittarelli et al., 2017). γ-Hydroxybutyrate (GHB), a powerful and rapid inhibitor of the central nervous system, has a powerful sedative effect (Adamowicz and Kała, 2010). It is purported to be a strength enhancer, euphoric, and aphrodisiac and is one of several medications reportedly used as a date rape drug (DRD) in crimes termed drug-facilitated sexual assault (DFSA). (Drasbek et al., 2006), (Schwartz et al., 2000), (Hall and Moore, 2008) The perpetrator chooses these drugs because they act rapidly, cause spontaneous muscle suppression and relaxation, and cause persistent total memory loss regarding events that occur under the influence of the drug. (DeVore and Sachs, 2011), (Trombley et al., 2020) GHB is eliminated from the plasma with a half-life of 30–50 min after ingestion. Only approximately 1–5% of the GHB dose can be recovered in the urine, and the detection window is relatively short (3–10 h) (Adamowicz and Kała, 2010). Comprehensive screening analysis of biological substances collected from victims of crimes involving a wide variety of substances used for criminal purposes revealed that low body fluid concentrations and long delays between incident and clinical examination make the detection of these drugs very difficult. (Kintz et al., 2001), (Palomino-Schätzlein et al., 2017), (Schröck et al., 2014)

Since endogenous GHB concentrations in plasma and urine can be easily detected with the highly sensitive analytical methods currently

* Corresponding author. Infectious Disease Research Center, Korea Research Institute of Bioscience and Biotechnology, Daejeon, 34141, Republic of Korea.
** Corresponding author. Biosystem Research Lab, Korea Institute of Toxicology, Daejeon, 34114, Republic of Korea.
E-mail addresses: wookkim@kitox.re.kr (W.-K. Kim), oskwon79@kribb.re.kr, oskwon7799@gmail.com (O.S. Kwon).
[1] These authors contributed equally to this work.

https://doi.org/10.1016/j.bios.2022.114195
Received 15 August 2021; Received in revised form 11 March 2022; Accepted 15 March 2022
Available online 18 March 2022
0956-5663/© 2022 Published by Elsevier B.V.

used for forensic testing, interpretation of the levels before and after GHB exposure has been of interest in recent years. (Purohit et al., 2020), (Kaufmann and Alt, 2007) There is no method to accurately detect whether GHB has been consumed; in particular, no method for the field-based determination of whether GHB has been consumed has yet been developed. To detect trace amounts of GHB after drug administration, a trained researcher must use equipment to analyze the urine and blood (Bertol et al., 2015), (Kaufmann and Alt, 2007), (Bertol et al., 2015), (Jürschik et al., 2012) For this reason, there is a great worldwide need to develop indirect analytical methods that can detect drugs used to commit sex crimes and prevent their administration. Most of the GHB detection methods proposed in recent papers use fluorescent substances or liquids. (Zhai et al., 2013), (Rodríguez-Nuévalos et al., 2020) These substances still have limitations for use in real-time field detection to ensure self-protection from DFSA. In most cases, specialized equipment is required for analyses involving a fluorescent sensor based on a low-molecular-weight compound (Table S1). Therefore, there is an urgent demand for self-protection products (SPPs) capable of fast, simple, accurate, real-time GHB monitoring in real life.

This study developed hydrogel-based SPPs for GHB detection that shows great potential for use in high-sensitivity, low-cost, portable systems that are simple to manufacture and can potentially be used for self-protection from DRDs. In particular, the recent focus has been on the development of various sensors using chemical/biological materials, and the chemical sensor developed in this study has the potential for use in SPPs. As shown in Scheme 1, a strategy that synergistically combines the GHB selectivity of 2-(3-bromo-4-hydroxystyryl)-3-ethylbenzothiazol-3-ium iodide (BHEI) and the high moisture content and controllable swelling and biocompatibility of hydrogels are used as the basis of in situ GHB detection. (Yoo et al., 2006), (Chai et al., 2017) In addition, when the color of a BHEI chemical receptor embedded in the hydrogel (BHEI-H) changes due to binding with GHB, the color of the entire hydrogel changes correspondingly (Puza et al., 2020). The color change of the SPPs can be observed in real-time with the naked eye, and at the same time, the risk posed by the detected concentration can be determined through detection of the color density using an application built into a smartphone for the colorimetric detection of GHB. (Cardoso et al., 2017), (Hellinger et al., 2020) This product has great potential as an SPP to interfere with sexual crime through the in situ detection of GHB.

2. Materials and methods

2.1. Materials

All reagents and solvents were purchased commercially and used as received. Iodoethane containing copper as a stabilizer, glycerol, acetonitrile, diethyl ether and ethanol were purchased from Sigma Aldrich Co., Ltd. 2-Methylbenzothiazole and poly(acrylic acid) (Carbopol-940) were purchased from Acros Organids Co., Ltd. 3-Bromo-4-hydroxybenzaldehyde was purchased from TCI Co., Ltd. Piperidine was purchased from Alfa Aesar Co., Ltd. γ-Hydroxybutyric acid (GHB, sodium salt) was purchased from Cayman Chemical Co.

2.2. Synthesis and characterization of BHEI

The synthesis was performed in two steps (not including column chromatography). First, 3-ethyl-2-methylbenzothiazol-3-ium iodide was prepared as follows: iodoethane (33.5 mmol) was added to a solution of 2-methylbenzothiazole (1 g, 6.7 mmol) in anhydrous acetonitrile. The mixture was heated under reflux at 90 °C for 20 h. After cooling, the solvent was evaporated in vacuo, and the residue was poured into diethyl ether. The precipitate was filtered under reduced pressure and washed several times with diethyl ether. The desired salt was dried in air to give a crystalline powder with a yield of 74%. In the second step, 3-ethyl-2-methylbenzothiazol-3-ium iodide (2 g, 6.55 mmol) was added to a solution of 3-bromo-4-hydroxybenzaldehyde (7.86 mmol) in ethanol (50 mL). Then, piperidine was added dropwise to the mixture at room temperature and stirred for 20 h. The precipitate that formed was filtered, washed with distilled water and ethanol several times to remove piperidine, and dried under vacuum to give a yellow powder with a yield of 34%. The ^{1}H and ^{13}C NMR spectra were recorded on a Bruker AVANCE III HD (9.4 T) 400 MHz spectrometer. Mass spectra were measured using a Bruker Daltonik (microTOF-QII) High Resolution Hybrid Tandem LC–MS/MS spectrometer at the Korea Advanced Institute of Science and Technology.

2.3. Statistical analysis

The normality and homogeneity of each variance were analyzed using the Shapiro–Wilk test and Levene's test, respectively. One-way analysis of variance (ANOVA) with Dunnett's test or the T3 test using SPSS 25 for Windows (SPSS, Chicago, IL, USA) was used to determine significant differences between the SC- and BHEI-exposed groups. For nonparametric data, the Kruskal–Wallis test was carried out. Differences

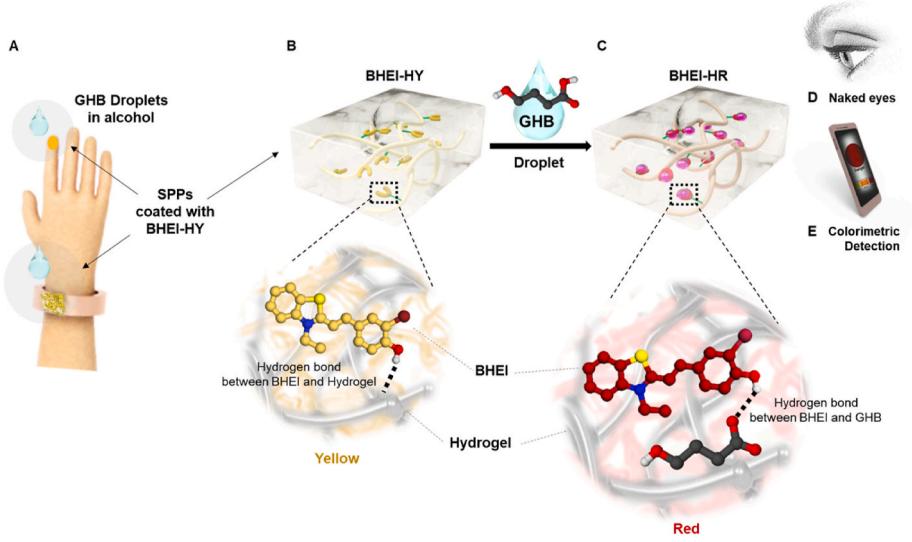

Scheme 1. Crimes caused by illegal use of γ-hydroxybutyric acid (GHB), are precipitously increasing. Therefore, there is an urgent demand for self-protection products (SPPs) capable of fast, facile, accurate, and real-time GHB monitoring for real life. In this study, we demonstrate in situ, real-time, and colorimetric GHB detection using various SPPs coated with the chemical receptor (2-(3-bromo-4-hydroxystyryl)-3-ethylbenzothiazol-3-ium iodide (BHEI))-embedded hydrogels. A strategy that synergistically combines the GHB selectivity of BHEI and the properties of hydrogels is used as the basis of the SPPs. The gel-type SPP can be coated on the human body or surrounding objects and is easy to remove (A). The BHEI-embedded hydrogel is yellow (BHEI-HY) (B) and changes to red after exposure to GHB droplets (BHEI-HR) (C). The color change is visible with the naked eye (D), and the concentration of GHB can be determined using a developed colorimetric detection-based smart phone application (E).

with $p < 0.05$ were considered statistically significant.

2.4. Toxicity screening using zebrafish embryo/larva model

Wild-type zebrafish (AB line, *Danio rerio*) and transgenic zebrafish lines (tg*(elavl3:eGFP)*, tg*(mbp:mGFP)*, and tg*(sox10:eGFP)*) were cultured in a temperature-controlled room (28 ± 0.5 °C) under a 14:10 h light:dark photoperiod in a fish breeding circulatory system at the Korea Institute of Toxicology (Daejeon, Korea). The three transgenic lines used in this study were obtained from the Zebrafish Center for Disease Modeling (ZCDM). Embryos were obtained from two or three pairs of adult male and female zebrafish. The embryos were collected and examined under a stereomicroscope to select normally fertilized embryos. Then, the embryos (≤3 hpf, hours post-fertilization) were exposed to test solutions (solvent control (SC) and 0.1, 1, 10, 100, 1000, and 10000 nM BHEI; and 1000 and/or 10000 nM BHEI-H) until 120 hpf. Test concentrations were chosen based on preliminary testing. Test solutions were prepared in E3 medium (0.292 g of NaCl, 0.013 g of KCl, 0.044 g of CaCl, and 0.081 g of $MgSO_4$ in Millipore filtered water (1 L)) and were replaced every 24 h with freshly made solutions. Dimethyl sulfoxide (DMSO, 0.1%) was used as the SC. All zebrafish exposures were conducted in accordance with the guidelines of the Institutional Animal Care and Use Committee (IACUC) of the Korea Institute of Toxicology (Protocol no. KIT-1907-0263, Approval date July 29, 2019).

The survival, hatching, and malformation of AB wild-type zebrafish embryos were observed and recorded every 24 h during the exposure period. The heart rates (beats per minute, bpm) were counted manually from 15 s recordings of AB wild-type zebrafish. Transgenic lines were used to examine the neurodevelopmental effects of BHEI. For tg*(mbp:mGFP)* and tg*(sox10:eGFP),* BHEI exposure was carried out only at the highest concentration (10000 Nm BHEI). Five zebrafish larvae (96 hpf and 120 hpf) per control and exposure group were anesthetized using tricane methane sulfonate (0.004% w/v), mounted on glass slides, and then observed under a fluorescence microscope (Zeiss AXIO imager.Z2). The brain and spinal cord widths of *the* tg*(elavl3:eGFP)* line were measured using ImageJ software.

2.5. Preparation and characterization of BHEI-HY

BHEI-HY was prepared by blending hydrogel with BHEI. First, poly (acrylic acid) (1 g) in pure glycerol (95 mL) was mixed under stirring (ca. 400 rpm) at 50 °C for 1.5 h, and then distilled water (ca. 5 mL) was added into the mixture at room temperature. After overnight incubation, 0.7% (w/w) trimethylamine (99.5%) was added to the mixture until the pH reached 6.5 to achieve high adhesion. In addition, the product (an adhesive hydrogel) was subjected to a cycle method, which consisted of freezing at 4 °C and thawing at 50 °C (10 times), to form a homogeneous hydrogel. Then, BHEI was added to the hydrogel to a final concentration of 10 mM. The evaluation of the mechanism of interaction between BHEI and GHB by virtual screening molecular docking and the modeling of BHEI and GHB were carried out with AutoDock. The 3D structures of BHEI and GHB were obtained in the sketch module of 3D ChemDraw. The structures were optimized and then used as input for comparison with the binding structure.

2.6. Titration of BHEI with GHB

Solutions of 10 mM BHEI and 1–10 mM GHB were prepared in 1% D_2O/DMSO-d_6. Increasing amounts of GHB were added to 10 mM BHEI solution for NMR analysis. UV–vis titration of a BHEI solution was carried out in DI water at concentrations of 0.01–1 mM. After that, increasing amounts of GHB from 0 to 10 mg/mL were added to the BHEI solution until saturation was reached, and a saturation plot was generated.

2.7. SEM imaging of the BHEI-HY

SEM imaging of BHEI-HY was performed to investigate the change in the internal structure of the hydrogel depending on the liquid containing GHB to which it was added. Specifically, the hydrogel was attached to a silicon wafer substrate, frozen in liquid nitrogen, and lyophilized in a drying system. The freeze-dried hydrogel was sputter-coated with 2 nm carbon using an EMS sputter coater. The hydrogel was imaged with a scanning electron microscope (FE-SEM (Sirion) with EDS by FEI) at 10 kV.

2.8. BHEI and BHEI-HY color change in beverages

BHEI: Alcoholic beverages were contaminated with GHB at 10 mg/mL. These solutions were mixed with BHEI (0.1 mM in DI water) in vials or well plates, and the color changes were observed immediately. BHEI-HY: BHEI-HY (5 mM) was coated on glass slides, nails, lipsticks, compacts, and gloves. Beverages containing 10 mg/mL GHB were dropped onto BHEI-HY, and the color changes were observed for 10 min. The process was carried out with several beverage samples, including beer, wine, whisky, vodka, cider, apple juice, sports drink, and soju.

Colorimetric measurement: The application for the colorimetric measurement of BHEI using a hydrogel probe and image processing was used as follows. First, the color change of BHEI was detected within 10 s by the naked eye, and then a spot on the samples was imaged with an application on a smartphone in a light-controlled area. The application was developed using Android Studio 4.1 as the development environment and Android 10 as the operating system. The software development kit was version 29, and the app development language was Android Java.

The application usage and analysis methods are as follows. The image is measured and captured by fixing the center of the display to the target sample (Sumriddetchkajorn et al., 2013). The captured screen is analyzed by focusing within a central circle on the measured screen to identify and quantify the pixels in the image (Helfer et al., 2017). First, the average red, green, and blue (RGB) intensities in the area are calculated, the calculated RGB value is converted to hue, saturation, and value (HSV), and the GHB concentration and risk are determined from the HSV value (Wang et al., 2017). When the application completes the analysis, the calculated results are shown on the display, and the text describing the stability, warning and risk appears depending on the amount of GHB.

3. Results and discussion

3.1. Synthesis and characterization of BHEI and BHEI-HY

BHEI and BHEI-HY were prepared from 2-methylbenzothiazole by the procedures described in Fig. 1. BHEI was synthesized from the starting material in two steps, and BHEI-HY was prepared from BHEI in a 1% poly(acrylic acid) solution in one step. The 3-bromo-4-hydroxybenzaldehyde moiety of BHEI binds to GHB to cause electron transfer (Zhai et al., 2014), and the electrons then interact with cyanine dye and cause a color change. BHEI and BHEI-HY are yellow in color and were characterized using ^{1}H and ^{13}C nuclear magnetic resonance (NMR) and mass spectrometry (Figs. S1–S5). (Liu et al., 2016)

3.2. Toxicity screening using a zebrafish model

No significant changes in survival, hatching, malformation, heartbeat, or neurodevelopment were observed in a zebrafish embryo/larvae model. All exposed embryos hatched successfully (Fig. 2a) and survived (data not shown) in the presence of up to 10000 nM BHEI. No deformities, i.e., curved spine, ocular malformations, or yolk edema, were observed. There were no significant differences in the heart rates of zebrafish larvae in the BHEI-exposed groups and the SC group (saline-

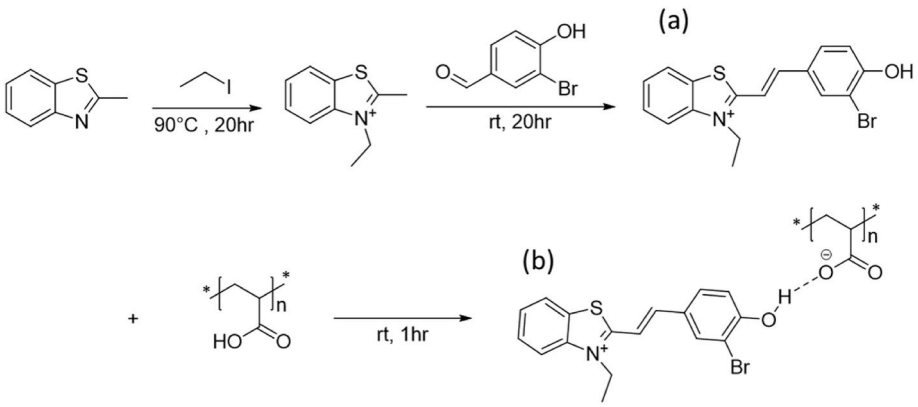

Fig. 1. Schematic of the preparation of BHEI-HY. Synthetic pathway for preparing BHEI (a) and BHEI-HY (b).

injected control group) (Fig. 2b). The heart rates of zebrafish larvae in the SC and BHEI-exposed groups were in the normal range for wild-type zebrafish (120–180 bpm at 72 hpf) according to a previous study (Sampurna et al., 2018).

To examine the neurodevelopmental effects of BHEI exposure, three transgenic lines, i.e., tg*(elavl3:eGFP),* tg*(mbp:mGFP)*, and tg*(sox10:eGFP),* were used. No significant changes in the neurodevelopment of zebrafish larvae after BHEI exposure were observed up to 10000 nM. Significant differences in brain width and spinal cord axon width in the tg*(elavl3:eGFP)* line were observed only between the SC group and the BHEI-exposed group at 10000 nM BHEI (Fig. 2c and **d**). As a neuronal marker, the gene elavl3 plays an important role in neuronal development and individual behavior (Guo et al., 2021). In this study, we also examined the myelination of oligodendrocytes and Schwann cells using the tg*(mbp:mGFP)* line. With this tg line, the differentiation of the anterior lateral line can be monitored. Myelin basic protein (mbp) can modulate myelin levels in the axons of the central nervous system in developing zebrafish (Buchtová et al., 2010). Myelination disruption can cause neurological diseases such as multiple sclerosis (Wang et al., 2019). There were no changes in myelination or differentiation of the anterior lateral line after BHEI exposure (Fig. 2e). The tg*(sox10:eGFP)* line used in this study labeled neural crest originating cells (Baumes et al., 2010). The fluorescence signals from the tg*(sox10:eGFP)* line were maintained after exposure to 10000 nM BHEI (Fig. 2f), which indicates that neural crest cells were not affected by BHEI exposure. Neurodevelopment experiments using three genetically modified lines confirmed that BHEI at up to 10000 nM caused no neurodevelopmental defects or damage. Toxicity assessment confirmed that BHEI had negligible harmful effects up to 10000 nM. Moreover, BHEI-H at concentrations up to 10000 nM (in 10% v/v poly(acrylic acid)) did not show any significant effects on survival, hatching, malformation, heartbeat, or neurodevelopment in the zebrafish embryo model (Fig. S6). This may indicate a low likelihood of toxic effects, allowing BHEI to be used in real life up to certain concentrations. The coefficient of variation (CV) was less than 5.5% in all toxicity screening tests.

3.3. Interaction of between BHEI and GHB

To confirm the degree of the GHB detection response of the developed BHEI, BHEI color change tests were performed with various beverages with GHB (Sansuk et al., 2020). First, GHB solutions from 0 to 10 mg/mL were prepared in DI water, and BHEI solutions from 4 to 500 μM were prepared in DI water on another plate. Through the color change experiment of BHEI according to volume, the two solutions were mixed in equal volumes (Fig. S7), and the color change was immediately monitored. As shown in Fig. 3a, as the concentration of GHB increased, the color of BHEI changed more clearly from yellow to red. When the concentration of BHEI was 120 μM or higher and the concentration of GHB was 0.01 mg/mL or higher, it was possible to visually distinguish between a solution without GHB and a solution to which GHB was added. In the UV–vis spectrum, the peak at 400 nm, in the yellow wavelength band, represents BHEI. This peak intensity was high before GHB was added and gradually decreased as the concentration of GHB increased. On the other hand, the intensity of the peak at 480 nm, in the red wavelength band, increased as the concentration of GHB increased (0–10 mg/mL). In addition, plotting the change in absorbance at 480 nm confirmed that saturation was achieved at a GHB concentration over 1 mg/mL (Fig. 3b).

The color change was evaluated in a variety of alcohols and beverages after adding GHB. Samples of each beverage without GHB and with 10 mg/mL GHB were prepared. Then, 0.25 mM BHEI was added, and the color change was observed. As shown in Fig. 3c, beverages without GHB retained their natural color or turned yellow from BHEI, while beverages with GHB turned red. The degree of color conversion varied depending on the beverage, but the same change from yellow to red was observed in all beverages. Detection was possible after simple mixing and verification, and the test was completed within 3 s. The peak of the UV–vis spectrum of beer shifted from 400 nm to 520 nm after the addition of BHEI. (Fig. 3d). (Yehia et al., 2020) The color change was verified through the change in the ultraviolet spectrum of the beverage, which was similar to the spectral change using water. These results show that BHEI can be used for the rapid visual detection of GHB in various beverages, and no additional instrumental analysis is required, showing the potential for use in a point-of-care system. We used non-pretreated beverages and confirmed that the substance of the beverage did not interfere with changes in BHEI or its reactions with GHB. Most of the GHB detection methods proposed in recent papers use fluorescent substances or liquids (Rodríguez-Nuévalos et al., 2020) or require specialized equipment for analyses involving a fluorescent sensor based on a low-molecular-weight compound (Zhai et al., 2013). Therefore, special equipment is not required to detect GHB using BHEI, and it has high sensitivity, high water solubility, and high selectivity to detect GHB with a small amount of BHEI, which is likely to be useable in real life.

We performed docking and NMR to confirm the hydrogen bonding and mechanism between the carboxyl acid of GHB and the –OH group of BHEI (Zhai et al., 2014) (Gu et al., 2017) (Satpathy et al., 2021). First, to determine the binding energy between GHB and BHEI, different configurations were calculated through the docking program Autodock (Shaikh et al., 2016). Additional simulation results are provided in Fig. S8. The most reasonable pose was identified with the highest score, and we chose the poses of GHB and BHEI based on docking scores, other literature, and experimental results. First, it was confirmed that the carboxyl residue of GHB and the hydroxyl residue of BHEI have a binding energy of - 4.3 kcal/mol. Among the various poses tested, the pose with 3.9 Å interbond distance was selected as the optimal pose for this study as a result of the supporting mechanism (Fig. 3e). Next, the

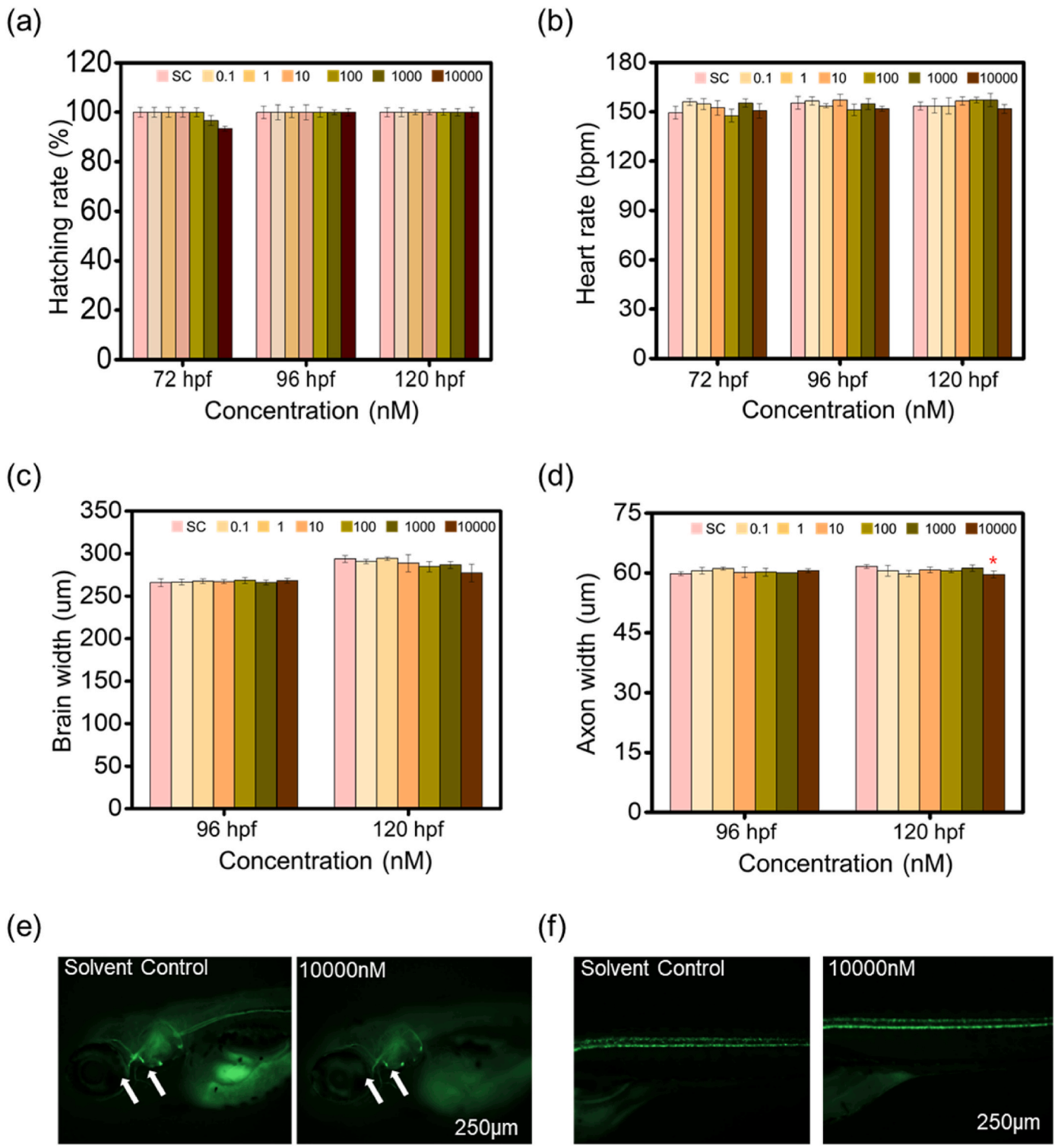

Fig. 2. Toxicity screening using zebrafish embryos. (a) Hatching rate (%), (b) heart rate (bpm), (c) brain width (μm) in tg*(elavl3:eGFP)*, (d) axon width (μm) in tg *(elavl3:eGFP)*, (e) fluorescence during the myelination of oligodendrocytes and Schwann cells using tg*(mbp:mGFP)* (white arrows: anterior lateral line), and (f) fluorescence in neural crest origin cells gener-ated using tg*(sox10:eGFP)*. B, C, D: Mean ± S.D, N = 5.

mechanism of the interaction between BHEI and GHB was further explored. Specific recognition of BHEI by GHB was established by NMR (Jang et al., 2017). Fig. 3f shows the 1H NMR spectrum of 10 mM BHEI alone and that of the same concentration of BHEI in the presence of various concentrations (0.1–1 equivalents) of GHB. The GHB equivalent was adjusted according to the concentration of BHEI, and a change in the proton resonance signal of BHEI was confirmed as the amount of GHB increased. We adjusted the molecular ratio of GHB to 1 equivalent of BHEI, and as the equivalent of GHB increased, the protons of BHEI, especially H7, H8, and H9, shifted upfield (1, 0.5, and 0.3 ppm, respectively). In particular, when the concentration of GHB exceeded that of BHEI by 0.5 equivalents, there was a noticeable peak shift. GHB was tested at concentrations from 0 to 1 equivalent of BHEI. The results are shown in Fig. S9 and suggest that the hydroxyl group of GHB forms a

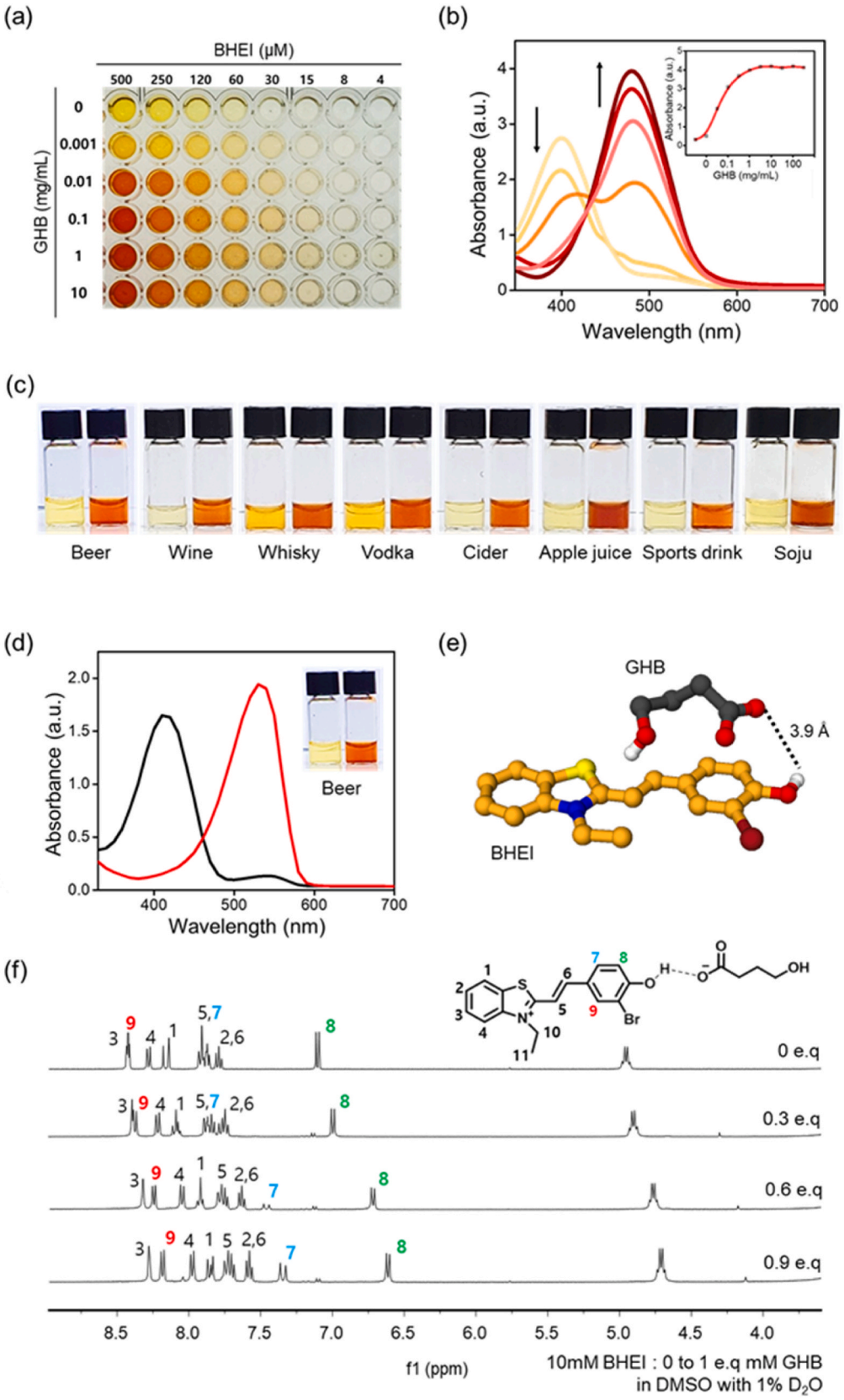

Fig. 3. Characterization of the interaction between BHEI and GHB. (a) Image showing the color change of BHEI (4–500 μM) after treatment with different concentrations of GHB (0–10 mg/mL) in DI water. (b) UV–vis spectra of BHEI (0.5 mM) with increasing concentrations of GHB (0–10 mg/mL) in DI water. (c) Image showing the color change of BHEI (0.12 mM) after treatment with GHB included beverages. (d) A graph comparing the absorption peaks of BHEI added to beer with and without GHB. (e) AutoDock simulation of BHEI conjugation with GHB showing the binding affinity and length between BHEI and GHB. (f) Partial 1H NMR spectra of BHEI (10 mM) upon addition of increasing equivalents of GHB in D_2O. (For interpretation of the references to color in this figure legend, the reader is referred to the Web version of this article.)

hydrogen bond with BHEI, and the formation of the hydrogen bond increases the strength of the electron transfer from GHB.

3.4. GHB detection experiment of BHEI-HY

Docking and NMR analyses confirmed that the hydroxyl groups and carboxylic acids of GHB and BHEI form hydrogen bonds, as shown in Fig. 3e and f. The mechanism of the subsequent reaction with poly (acrylic acid) is shown in Fig. 4a. Poly(acrylic acid) is a polymer in which a carboxylic acid is connected to a carbon backbone. When it is antagonized with BHEI, the hydroxyl group of poly(acrylic acid) and the hydroxyl group connected to the benzene ring in BHEI form a bond (Xu et al., 2019). Then, when GHB is added, a color change occurs in the hydrogel because of the reaction between GHB and BHEI. We measured the binding energy between GHB and poly(acrylic acid) through Autodock; the maximum was - 1.7 kcal/mol, and the minimum was - 1.5 kcal/mol. These values reflect a weak bond compared to - 4.7 kcal/mol between GHB and BHEI, and the distances of 4.1 Å and 5.5 Å between BHEI and poly(acrylic acid) (Fig. S10) indicate weaker hydrogen bonding than that between BHEI and GHB (3.9 Å). Therefore, when GHB is added to the polymer in which BHEI is embedded, the color of BHEI changes from yellow to red due to the strong reaction between GHB and BHEI. We analyzed SEM images before and after the reaction to confirm that BHEI reacts stably in poly(acrylic acid). An SEM image of the hydrogel (Fig. 4b) is shown below the stepwise schematic of the hydrogel preparation. The following hydrogels are presented from left to right in the image: 1% poly(acrylic acid) alone, BHEI-embedded hydrogel before GHB addition (BHEI-HY), and BHEI-embedded hydrogel after GHB addition (BHEI-HR). These images show that the three types of hydrogels maintained the same pore shape. First, the control group (1% poly(acrylic acid)) made of a nonreactive precursor formed a porous structure with pores of 10 mm. Then, when 5 mM BHEI was dissolved in water and mixed into the hydrogel, a stable blended gel formed due to the electrical attraction and hydrogen bonding between the two substances. In the second type of hydrogel mixed with BHEI, the shape of the pores was maintained, and the surrounding substance containing BHEI was transformed into an undefined film. Finally, after GHB was added to BHEI-HY, the texture changed while the shape of the pores was maintained, with both BHEI and GHB surrounding the pores. This suggests that the swelling of BHEI-HY is controlled by the maintenance of the shape of its pores after the addition of GHB and that GHB is captured through strong binding with BHEI around the pores. Therefore, this hydrogel can be coated on various surfaces, such as the human body and substances for SPPs; the hydrogel provides a good coating on many types of surfaces and can be easily removed by using water.

In addition, the hydrogel, which is tightly bonded after freeze-thawing, can protect the reaction from exposure to the external environment. BHEI-HY mostly consists of glycerol, has a very high viscosity between pH 5 and 8.5 (Fig. S11), and was found to be very stable both at room temperature and at 4 °C for 30 days (Fig. S12). In addition, the color change of BHEI-HY was observed for 30 days by the 0, 1, and 10 mM of GHB. As a result, the same color change and high stability of BHEI-HY for each concentration of GHB were confirmed (Fig. S13). To assess the performance of the produced hydrogel platform, a 1% poly (acrylic acid) solution containing 5 mM BHEI was first coated on bracelets or around objects, and a beverage with 10 mg/mL GHB was prepared (Fig. 4c). There was no color change of the BHEI-HY at the location where a beverage without GHB was dropped, but a change from yellow to red (BHEI-HR) occurred within 1 min at the location where a beverage with GHB was dropped. A variety of products that can be coated with hydrogel were tested, and GHB was detected rapidly due to the high adhesion and absorption of the hydrogel. This experiment was carried out for up to 10 min, and the greatest color change from yellow (BHEI-HY) to red (BHEI-HR) was observed within 3 min, with no further color change up to 10 min. The results of various experiments on the color change are shown in Fig. S14. Because the hydrogel is transparent and adhesive, it can be used to detect GHB secretly and easily at crime scenes where drugs were used, demonstrating its potential as an SPP that could be used to prevent crimes related to GHB.

These results imply that our BHEI-HY holds promise for application to hydrogel-based GHB detection. Therefore, BHEI-HY is highly useable in real life compared to the existing methods for GHB detection using liquids(Zhai et al., 2014)(Rodríguez-Nuévalos et al., 2020). and has potential an SPP, especially at crime scenes.

3.5. Colorimetric detection application demonstration

We developed a smartphone application using the Android system for the colorimetric detection of GHB (Fig. 5) (Seo et al., 2019). This program was developed to observe BHEI-HR whose color had changed due to exposure to a beverage with GHB and to measure the sensitivity and risk according to the concentration more accurately than is possible by eye. The colors in the photos are classified using the RGB-HSV formula, and the detailed formula is attached to the supporting material.

To test the performance of the application, 5 mM BHEI-embedded BHEI-HY was first coated on a substrate, 10 mg/mL GHB was dropped onto BHEI-HY, and the color change was confirmed with the application. The result was completed within 3 s. SAFETY appeared on the screen when GHB was absent, and DANGER appeared where GHB was dropped. Where 1 mg/mL to 5 mg/mL of GHB was dropped, ALERT appeared. The colors in the photos are classified using the following formula. First, the application retrieves the red (R), green (G), and blue (B) values in the range 0–1 and then retrieves the largest and smallest values of each (eqs (1)–(6)). Next, we obtain hue (H), saturation (s), and value (V). To do this, we look at the largest of the R, G, B, values (eq (7)). S is the difference between the maximum and minimum color channel values divided by the brightness V. If V is 0, the resulting saturation is 0 (eq (8)). The brightness, V, is based on the brightest color channel (eq (9)). Hue (H), saturation (S), brightness or value (V), red (R), green (G), and blue (B) are obtained as described in eqs (1)–(9), below.

$$R' = R/255 \tag{1}$$

$$G' = G/255 \tag{2}$$

$$B' = B/255 \tag{3}$$

$$Cmax = \max(R', G', B') \tag{4}$$

$$Cmin = \min(R', G', B') \tag{5}$$

$$\triangle = Cmax - Cmin \tag{6}$$

Hue Calculation:

$$H = \begin{cases} 60^\circ X \left(\frac{G' - B'}{\triangle} mod 6\right), & Cmax = R' \\ 60^\circ X \left(\frac{B' - R'}{\triangle} + 2\right), & Cmax = G' \\ 60^\circ X \left(\frac{R' - G'}{\triangle} + 4\right), & Cmax = B' \end{cases} \tag{7}$$

Saturation calculation:

$$S = \begin{cases} 0, & Cmax = 0 \\ \left(\frac{\triangle}{Cmax}\right), & Cmax \neq 0 \end{cases} \tag{8}$$

Value calculation:

$$V = Cmax \tag{9}$$

The photograph shows a comparison of the color of the actual sample and of the sample measured with the application. To verify the effectiveness of the application, we conducted 10 experiments. A total of 6

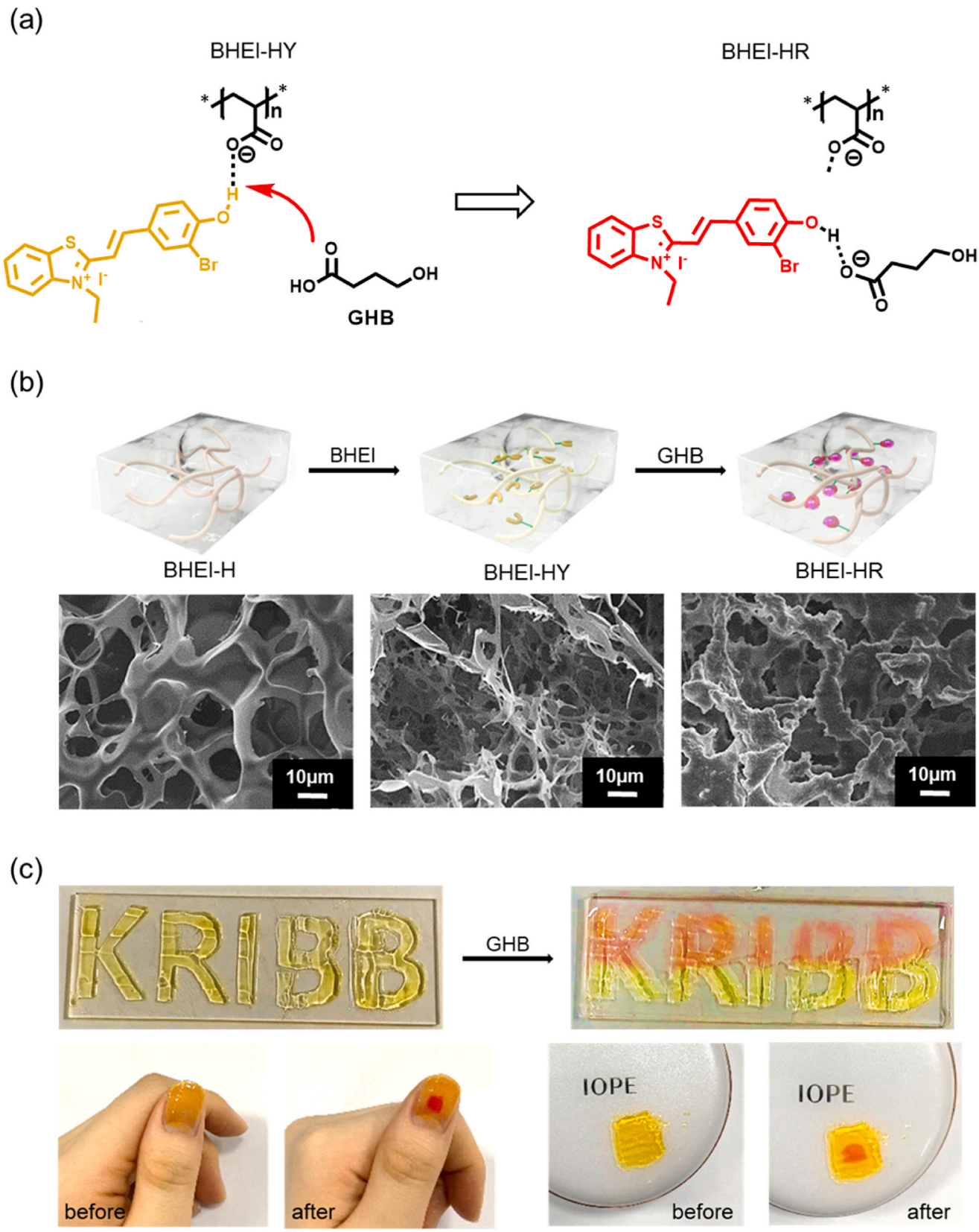

Fig. 4. Mechanism of GHB detecting of BHEI functionalized hydrogel. (a) Mechanisms of BHEI conjugation with poly(acrylic acid) and BHEI-HY interaction with GHB. (b) Schematic and SEM images showing the color change of BHEI-HY to BHEI-HR. The left SEM image is a polymer containing 1% poly(acrylic acid), the center image shows the addition of BHEI to 1% poly(acrylic acid) and the color change to yellow, and the right image shows the color change from yellow to red after dropping GHB on BHEI-HY. (c) Image of the color change of BHEI-HY (10 mM) to BHEI-HR after exposure to GHB included beverages. (For interpretation of the references to color in this figure legend, the reader is referred to the Web version of this article.)

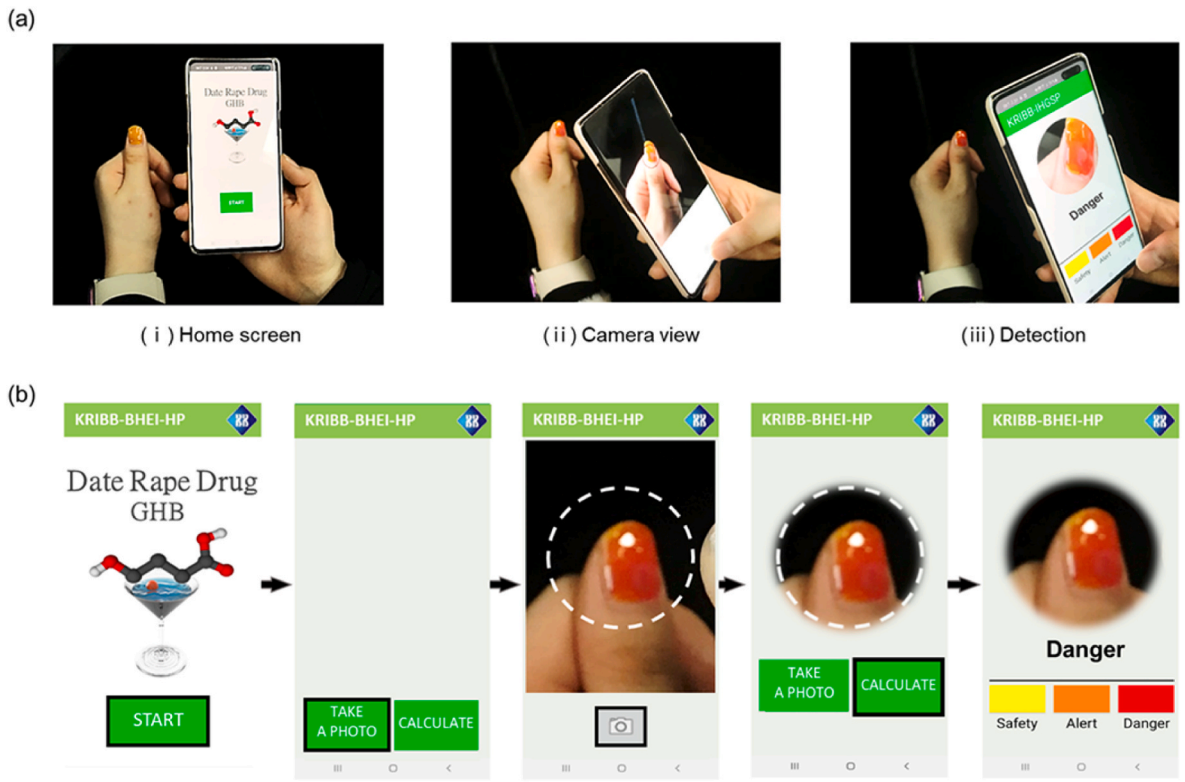

Fig. 5. Colorimetric detection application for color change of BHEI (a) Simulation of detecting the GHB concentration with a colorimeter on a smartphone. Proposed application for the detection of GHB on a smartphone. (b) 1. Opening the page. 2. Select the page to take a photograph. 3. Camera view with a focus on the sample and captured raw image. 4. Processing the im-age using a created mask (total pixel number shown below). 5. Calculated degree of risk for the sum of the pixel intensity values. (For interpretation of the references to color in this figure legend, the reader is referred to the Web version of this article.)

out of 10 correct results were obtained when the color checked was checked with eyes, but when the color change was detected with the application, all 10 out of 10 results were correct. Thus, the potential of the application as an SPP has been confirmed, as it can be used in places where color identification is difficult or by people for whom visual detection is difficult (Fig. S15).

4. Conclusions

In summary, we have developed a highly sensitive GHB detection method using a BHEI-embedded hydrogel for SPPs that can selectively detect GHB in various beverages. To develop this in situ GHB detection system, we first identified the site and mechanism by which GHB recognizes BHEI and confirmed the functionalized stability and safety of using hydrogels for the application of BHEI. The highly absorbable hydrogel speeds up the detection and increases the sensitivity and selectivity: only 100 μM to 5 mM BHEI is needed to detect 10 mg/mL GHB, a typical concentration found at crime scenes. In addition, we successfully developed an application for the real-time detection of color changes visible to the naked eye for the rapid detection of GHB. Although the accuracy of the concentration measurement is lower than that of the existing GC method, the developed system can be used for detection before drug use, thus showing potential as an SPP that can prevent serious sex crimes. This viable system is an inexpensive, simple and highly sensitive and selective GHB detection product for preventive applications and a new alternative to current drug detection.

CRediT authorship contribution statement

Siyoung Ha: Formal analysis, Writing – original draft, Writing – review & editing. **Jinyeong Kim:** Formal analysis, Writing – original draft, Writing – review & editing. **Chul Soon Park:** Resources. **Sangwoo Lee:** Formal analysis, Writing – original draft, Writing – review & editing. **Donggon Yoo:** Formal analysis. **Kyung Ho Kim:** Investigation. **Sung Eun Seo:** Investigation. **Seon Joo Park:** Investigation. **Jai Eun An:** Investigation. **Hyin Seok Song:** Methodology, Investigation. **Joonwon Bae:** Methodology, Investigation. **Woo-Keun Kim:** Project administration. **Oh Seok Kwon:** Supervision, Project administration, Writing – original draft, Writing – review & editing.

Declaration of competing interest

The authors declare that they have no known competing financial interests or personal relationships that could have appeared to influence the work reported in this paper.

Acknowledgments

This work was supported by the Technology Innovation Program (Project No. 20012362) funded by the Ministry of Trade, Industry & Energy (MOTIE, Korea); the Research Program to Solve Urgent Safety Issues of the National Research Foundation of Korea(NRF) funded by the Korean government (Ministry of Science and ICT(MSIT)) (NRF-2020M3E9A1111636); Korea Institute of Planning and Evaluation for Technology in Food, Agriculture and Forestry(IPET) and Korea Smart Farm R&D Foundation(KosFarm) through Smart Farm Innovation Technology Development Program, funded by Ministry of Agriculture, Food and Rural Affairs(MAFRA) and Ministry of Science and ICT(MSIT), Rural Development Administration(RDA) (421020–03); Korea Environment Industry & Technology Institute (KEITI) through Core Technology Development Project for Environmental Diseases Prevention and Management, funded by Korea Ministry of Environment (MOE) (RE2021003310003); National R&D Program of National Research Foundation of Korea(NRF) funded by Ministry of Science and ICT

(2021M3H4A407927 6); and the Korea Research Institute of Bioscience and Biotechnology(KRIBB) Research Initiative Program(1711134045, 1711134067).

Appendix A. Supplementary data

Supplementary data to this article can be found online at https://doi.org/10.1016/j.bios.2022.114195.

References

Adamowicz, P., Kała, M., 2010. Forensic Sci. Int. 198, 39–45.
Baumes, L.A., Sogo, M.B., Montes-Navajas, P., Corma, A., Garcia, H., 2010. Chem. Eur J. 16, 4489–4495.
Bertol, E., Mari, F., Vaiano, F., Romano, G., Zaami, S., Baglìo, G., Busardò, F.P., 2015. Drug Test. Anal. 7, 376–384.
Buchtová, M., Kuo, W.P., Nimmagadda, S., Benson, S.L., Geetha-Loganathan, P., Logan, C., Au-Yeung, T., Chiang, E., Fu, K., Richman, J.M., 2010. Dev. Dynam. 239, 574–591.
Cardoso, L.A.C., Karp, S.G., Vendruscolo, F., Kanno, K.Y.F., Zoz, L.I.C., Carvalho, J.C., 2017. We Are IntechOpen , the World ' s Leading Publisher of Open Access Books Built by Scientists , for Scientists TOP 1 %, pp. 125–141. Intech.
Chai, Q., Jiao, Y., Yu, X., 2017. Gels 3, 6.
DeVore, H.K., Sachs, C.J., 2011. Emerg. Med. Clin. 29, 605–620.
Drasbek, K.R., Christensen, J., Jensen, K., 2006. Acta Neurol. Scand. 114, 145–156.
Gu, Q., Su, P., Xia, Y., Yang, Z., Trindle, C.O., Knee, J.L., 2017. Physical Chemistry Chemical Physics.
Guo, S.Y., Zhang, Y., Zhu, X.Y., Zhou, J.L., Li, J., Li, C.Q., Wu, L.R., 2021. J. Appl. Toxicol. 41, 549–560.
Hall, J.A., Moore, C.B.T., 2008. J. Forensic Legal Med. 15, 291–297.
Helfer, G.A., Magnus, V.S., Böck, F.C., Teichmann, A., Ferrão, M.F., Da Costa, A.B., 2017. J. Braz. Chem. Soc. 28, 328–335.
Hellinger, R., Silva, V.B., Orth, E.S., 2020. Pure Appl. Chem. 92, 601–616.
Jang, Y., Jang, M., Kim, H., Lee, S.J., Jin, E., Koo, J.Y., Hwang, I.C., Kim, Y., Ko, Y.H., Hwang, I., Oh, J.H., Kim, K., 2017. Inside Chem. 3, 641–651.
Jürschik, S., Agarwal, B., Kassebacher, T., Sulzer, P., Mayhew, C.A., Märk, T.D., 2012. J. Mass Spectrom. 47, 1092–1097.
Kaufmann, E., Alt, A., 2007. Forensic Sci. Int. 168, 133–137.
Kintz, P., Goullé, J.P., Cirimele, V., Ludes, B., 2001. Clin. Chem. 47, 2033–2034.
Liu, B., Wang, H., Yang, D., Tan, R., Zhao, R.R., Xu, R., Zhou, Z.J., Zhang, J.F., Zhou, Y., 2016. Dyes Pigments 133, 127–131.
Palomino-Schätzlein, M., Wang, Y., Brailsford, A.D., Parella, T., Cowan, D.A., Legido-Quigley, C., Pérez-Trujillo, M., 2017. Anal. Chem. 89, 8343–8350.
Purohit, S., Pandey, G., Tharmavaram, M., Rawtani, D., Mustansar Hussain, C., 2020. Technology Forensic Sci. 221–238.
Puza, F., Zheng, Y., Han, L., Xue, L., Cui, J., 2020. Polym. Chem. 11, 2339–2345.
Rodríguez-Nuévalos, S., Costero, A.M., Arroyo, P., Saéz, J.A., Parra, M., Sancenón, F., Martínez-Máñez, R., 2020. Chem. Commun. 56, 12600–12603.
Sampurna, B.P., Audira, G., Juniardi, S., Lai, Y.H., Hsiao, C. Der, 2018. Inventions 3, 1–11.
Sansuk, S., Juntarakod, P., Tongphoothorn, W., Sirimungkala, A., Somboon, T., 2020. Food Control 110, 107042.
Satpathy, S., Patra, A., Hussain, M.D., Kazi, M., Aldughaim, M.S., Ahirwar, B., 2021. PLoS ONE 16.
Schröck, A., Hari, Y., König, S., Auwärter, V., Schürch, S., Weinmann, W., 2014. Drug Test. Anal. 6, 363–366.
Schwartz, R.H., Milteer, R., Lebeau, M.A., 2000. South. Med. J. 93, 558–561.
Seo, S.E., Tabei, F., Park, S.J., Askarian, B., Kim, K.H., Moallem, G., Chong, J.W., Kwon, O.S., 2019. J. Ind. Eng. Chem. 77, 1–11.
Shaikh, N., Sharma, M., Garg, P., 2016. Mol. Biosyst. 12.
Sumriddetchkajorn, S., Chaitavon, K., Intaravanne, Y., 2013. Sensor. Actuator. B Chem. 182, 592–597.
Tittarelli, R., Pichini, S., Pedersen, D.S., Pacifici, R., Moresco, M., Pizza, F., Busardò, F.P., Plazzi, G., 2017. Forensic Sci. Int. 274, 70–74.
Trombley, T.A., Capstick, R.A., Lindsley, C.W., 2020. ACS Chem. Neurosci. 11.
Wang, F., Lu, Y., Yang, J., Chen, Y., Jing, W., He, L., Liu, Y., 2017. Analyst 142, 3177–3182.
Wang, H., Zhou, L., Meng, Z., Su, M., Zhang, S., Huang, P., Jiang, F., Liao, X., Cao, Z., Lu, H., 2019. Environ. Pollut. 255, 113218.
Xu, L., Wang, C., Cui, Y., Li, A., Qiao, Y., Qiu, D., 2019. Sci. Adv. 5.
Yehia, A.M., Farag, M.A., Tantawy, M.A., 2020. Anal. Chim. Acta 1104, 95–104.
Yoo, J.W., Dharmala, K., Lee, C.H., 2006. Int. J. Pharm. 309, 139–145.
Zhai, D., Agrawalla, B.K., Fronia Eng, P.S., Lee, S.C., Xu, W., Chang, Y.T., 2013. Chem. Commun. 49, 6170–6172.
Zhai, D., Elton Tan, Y.Q., Xu, W., Chang, Y.T., 2014. Chem. Commun. 50, 2904–2906.